

An adaptive dimension reduction algorithm for latent variables of variational autoencoder

Yiran Dong and Chuanhou Gao, *Senior Member, IEEE*

Abstract—Constructed by the neural network, variational autoencoder has the overfitting problem caused by setting too many neural units, we develop an adaptive dimension reduction algorithm that can automatically learn the dimension of latent variable vector, moreover, the dimension of every hidden layer. This approach not only apply to the variational autoencoder but also other variants like Conditional VAE(CVAE), and we show the empirical results on six data sets which presents the universality and efficiency of this algorithm. The key advantages of this algorithm is that it can converge the dimension of latent variable vector which approximates the dimension reaches minimum loss of variational autoencoder(VAE), also speeds up the generating and computing speed by reducing the neural units.

Index Terms—Variational autoencoder, latent variable, dimension reduction, Lagrange loss, convergence



1 INTRODUCTION

VARIATIONAL autoencoder(VAE) [1] is a famous generative model which can generate specific distribution compares to GAN [2], VAE contains the encoder and decoder and they are constructed from the neural networks, the encoder encodes the data into latent variables, then the decoder decodes the latent variables into a new data.

Dimension reduction is an important technique for training models in machine learning, dimension reduction is often used on the data set as a preliminary step before feeding these data to the machine learning models. For most dimension reduction algorithms, they are nothing but various projections, including principal component analysis(PCA) [3], the most widely used technique in dimension reduction. For example, the data is on the D -dimensional space, we project the data into the L -dimensional space, where $L < D$. The aim of dimension reduction is mainly to avoid the increasing complexity in models with the increasing dimension of data, i.e. the curse of the dimensionality. Different from these traditional techniques, the adaptive dimension reduction algorithm in this paper reduces the dimension not by projection but by judging each feature, whether it contains too much noise. Moreover, it learns the dimension it needs to reduce.

We aim to decrease the dimension of the latent variable vector, the dimension reduction on latent variables can improve the model on test set by wiping off useless information to denoise and speed up the forward process. We can also prove that the loss on test set related to dimension of latent variable is convex, and our algorithm have done well in the experiments on finding the solution of this convex problem. Details on the convexity are discussed in later sections.

The improvement on VAE has appeared, for example the conditional variational autoencoder(CVAE) [4], [5] considers the label as hidden variables, the Stein VAE [6], [7] presents a new approach to maximize the ELBO and update the parameters of network and the Beta VAE. [8] These various variants of VAE all

have the encoder, decoder and the latent variables, so the analysis in VAE can be used on these variants similarly. In the experiments, we mainly use our algorithm on VAE and CVAE.

We also present a new converge method, n -steps optimization, which gets inspiration from sequential minimal optimization(SMO) [9]. The SMO is mainly to solve the duality problem in support vector machines(SVM), and the thought behind it also serves well in solving the Lagrangian equation we confront in the adaptive dimension reduction algorithm.

Further, one may require many layers to achieve the goal, the adaptive dimension reduction algorithm also can learn the dimension of every hidden layers, in this situation, we may not find the model can achieve the minimum loss on testing set (but good enough), but we can accelerate the forward speed dramatically by deleting the neural units.

The rest of the paper is organized as follows. Section 2 presents some preliminaries about VAE and CVAE. In Section 3, our main work, the adaptive dimension reduction algorithm as well as its convergence and application, is presented. This is followed by some experimental studies of the proposed algorithms in Section 4. Finally, Section 5 concludes the paper.

2 PRELIMINARIES

In this section we will give a short introduction on VAE and CVAE [10], and then present the assumption that is used for algorithms development.

2.1 VAE and CVAE

VAE is a kind of graphical model, whose main purpose is to minimize the \mathcal{KL} divergence between the true posterior distribution and the learned one on the data set.

Let $\mathbb{D} = \{\mathbf{x} \in \mathbb{R}^N\}$ represent a data set, and $\mathbf{z} \in \mathbb{R}^m$ represent the latent variable vector in VAE, then the mentioned \mathcal{KL} divergence is defined as (essentially, the expectation calculation)

$$\mathcal{KL}[Q(\mathbf{z}|\mathbf{x}) \parallel P(\mathbf{x}|\mathbf{z})] = E_{Q(\mathbf{z}|\mathbf{x})}[\log Q(\mathbf{z}|\mathbf{x}) - \log P(\mathbf{z}|\mathbf{x})], \quad (1)$$

where $Q(\mathbf{z}|\mathbf{x})$ and $P(\mathbf{x}|\mathbf{z})$ denote the true posterior distributions and learned one on \mathbb{D} , respectively. They are usually called the

• Y. Dong and C. Gao are with the School of Mathematical Sciences, Zhejiang University, Hangzhou 310027, China.
E-mail: {22035082, gaouchou}@zju.edu.cn

encoder and decoder of VAE. By utilizing $P(\mathbf{x})$ and applying the Bayes rule, the above definition can be rewritten as

$$\begin{aligned} & \log P(\mathbf{x}) - \mathcal{KL}[Q(\mathbf{z}|\mathbf{x}) \parallel P(\mathbf{x}|\mathbf{z})] \\ & = E_Q[\log P(\mathbf{x}|\mathbf{z})] - \mathcal{KL}[Q(\mathbf{z}|\mathbf{x}) \parallel P(\mathbf{z})], \end{aligned} \quad (2)$$

which is the core formula in VAE.

where $P(\mathbf{z})$ is normal distribution, $P(\mathbf{x}|\mathbf{z})$ and $Q(\mathbf{z}|\mathbf{x})$ are called as decoder and encoder, the usual choices are set as Gaussian distributions:

$$Q(\mathbf{z}|\mathbf{x}) = \mathcal{N}(\mu(\mathbf{x}), \Sigma(\mathbf{x})) \quad P(\mathbf{x}|\mathbf{z}) = \mathcal{N}(f(\mathbf{z}), \sigma^2). \quad (3)$$

And \mathbf{z} is the latent variables vector we mentioned before, we want to decrease the dimension of \mathbf{z} as much as possible.

Note that the , since it wants to mimic the true posterior distribution $Q(\mathbf{z}|\mathbf{x})$ by using the Gaussian posterior distribution $P(\mathbf{x}|\mathbf{z})$ with the mean, $f(\mathbf{z})$ constructed by the deep neural network(DNN), and the constant variance σ^2 . However, we assume the variables are all independent in Gaussian posterior distribution, this technique is called *meanfield*. But what if we use more complicated graph to mimic the actual posterior distribution? Here leads to the Structure VAE(SVAE). [11]

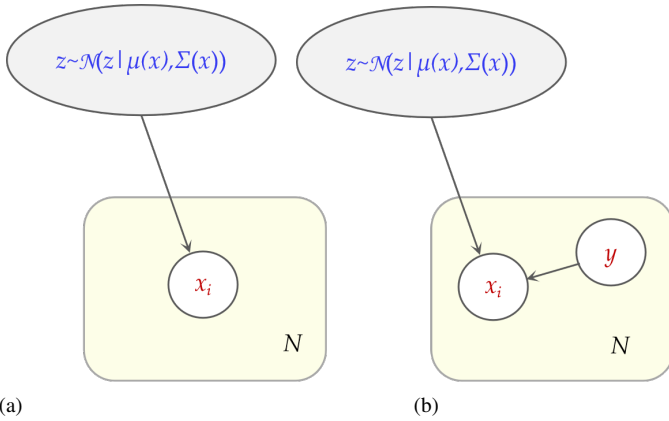


Fig. 1: (a) The graph structure of VAE, the N represents the dimension of X (b) The graph structure of CVAE. The x_i are the features in \mathbf{x}

From the figure 1, the N in the square is the dimension of the X , since the \mathbf{z} is a known variables vector after the encoding process, the $\{x_i\}$ are independent with each other when \mathbf{z} is known, where $\{x_i\}$ are the features of \mathbf{x} [12].

Due to the \mathcal{KL} divergence is nonnegative, the right of formula (2) is a lower bound of likelihood function and is called evidence lower bound(ELBO). After all, what we learn is a approximation of maximum likelihood estimation.

CVAE takes the training set \mathbf{X} and their labels \mathbf{Y} into consideration (figure 3). Let y be the label of a data point \mathbf{x} , CVAE places the encoder and decoder as

$$Q(\mathbf{z}|\mathbf{x}, \mathbf{y}) = \mathcal{N}(\mu(\mathbf{x}, \mathbf{y}), \Sigma(\mathbf{x}, \mathbf{y})) \quad P(\mathbf{x}|\mathbf{z}, \mathbf{y}) = \mathcal{N}(f(\mathbf{z}, \mathbf{y}), \sigma^2), \quad (4)$$

it can be proved that the loss is the ELBO of $P(\mathbf{x}|\mathbf{z}, \mathbf{y})$. Apparently, CVAE contains the information of every labels and can generate better images of different category.

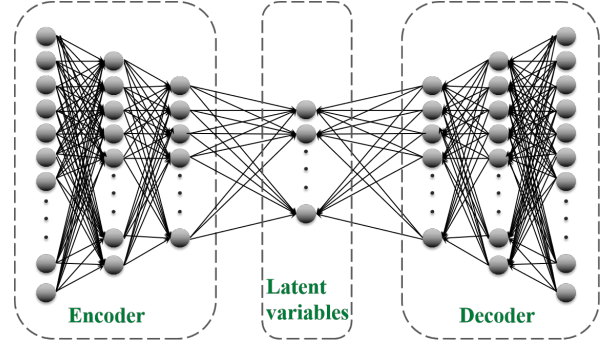


Fig. 2: VAE with 3 layers encoder and 3 layers of decoder.

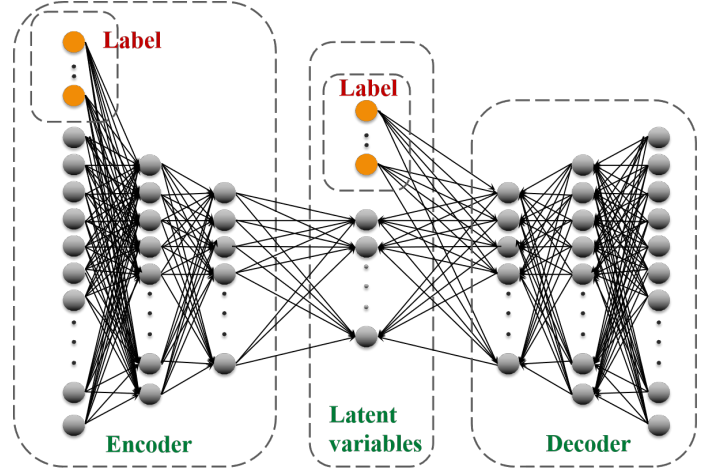


Fig. 3: CVAE with 3 layers encoder and 3 layers of decoder.

2.2 Assumption

In order to facilitate the design of dimension reduction algorithms, the following assumption is made for VAE and CVAE.

Denote the training precision loss function by $h_{\mathbf{z}}$, where \mathbf{z} is identified as an m -dimensional latent variable vector in the model \mathcal{M} .

Assumption: Let \mathbf{v} and \mathbf{w} be the $m_{\mathbf{v}}$ -dimensional latent vector and $m_{\mathbf{w}}$ -dimensional latent vector and $m_{\mathbf{v}} < m_{\mathbf{w}}$, for small ϵ , if

$$\begin{aligned} h_{\mathbf{v}} - h_{\mathbf{z}} &\leq \epsilon \\ h_{\mathbf{w}} - h_{\mathbf{z}} &\leq \epsilon \end{aligned}$$

Then $h_{\mathbf{v}} < h_{\mathbf{w}}$ \square

It should be noted that the assumption is reasonable to a certain extent. For small ϵ , the units we discard are useless information and can be seen as noise, $m_{\mathbf{w}} < m_{\mathbf{v}}$ states that VAE with \mathbf{v} deletes more noise and should have better loss on training and test set. This means that the above assumption is reasonable. Another point needed to be noted is that the current assumption can work not only for VAE and CVAE, but for other autoencoder models.

3 ADAPTIVE DIMENSION REDUCTION ALGORITHM

In this section, we will develop the adaptive dimension reduction algorithm for latent variables in VAE and CVAE, and also give the corresponding theoretical analysis.

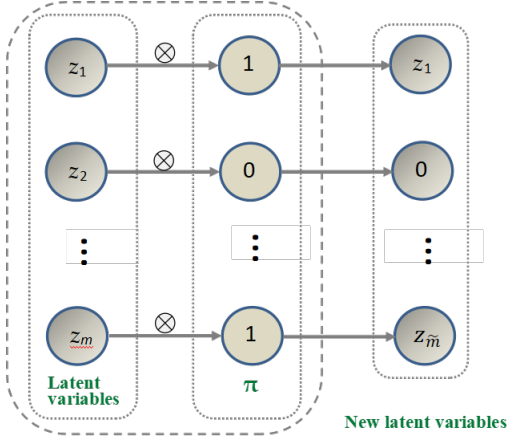


Fig. 4: Schematic of generating new latent variables by π .

3.1 Lagrange Loss

In the process of algorithm design, we expect to find a model with latent variables $\tilde{\mathbf{z}}$ that has the minimum precision loss compared to the original model with latent variables \mathbf{z} . Mathematically, it can be modelled as, for small enough $\varepsilon \geq 0$,

$$h_{\tilde{\mathbf{z}}} - h_{\mathbf{z}} \leq \varepsilon. \quad (5)$$

We introduce a special m -dimensional vector π , whose elements are ones or zeros, to build a new model as

$$h_{\pi \otimes \mathbf{z}} - h_{\mathbf{z}} \leq \varepsilon, \quad (6)$$

where the symbol \otimes represents the element-wise multiplication. From the expression $\pi \otimes \mathbf{z}$, we could say the latent variable z_i is activated if the corresponding $\pi_i = 1$; otherwise, z_i is inactivated, and the information about z_i cannot pass to the decoder and is seen as noise. Fig. 4 exhibits the generation process of new latent variables utilizing π . For the new model of (6), we have

Lemma 1. *If $\sum_{i=1}^m \pi_i = \tilde{m}$ in (6), then (5) holds true from (6).*

Proof. If $\sum_{i=1}^m \pi_i = \tilde{m}$, $\pi \otimes \mathbf{z}$ will define a group of new latent variables, which corresponds to a new model including \tilde{m} latent variables, but shares the same parameters with \mathcal{M} . Note that the model $\tilde{\mathcal{M}}$ having training precision loss function $h_{\tilde{\mathbf{z}}}$ has been trained to possess better training precision in all models with \tilde{m} latent variables, so $h_{\tilde{\mathbf{z}}} \leq h_{\mathbf{z} \otimes \pi}$, i.e., the result is true. \square

The following task for the algorithm development is to minimize $\sum_{i=1}^m \pi_i$ satisfying (6). Based on (2), we take the loss function as the minus of ELBO, i.e.,

$$h_{\pi \otimes \mathbf{z}} = -E_Q[\log P(\mathbf{x}|\pi \otimes \mathbf{z})] + \mathcal{KL}[Q(\pi \otimes \mathbf{z}|\mathbf{x}) \| P(\pi \otimes \mathbf{z})], \quad (7)$$

where

$$\begin{cases} Q = Q(\pi \otimes \mathbf{z}|\mathbf{x}) = \prod_i^m \mathcal{N}(z_i|\mu_i(\mathbf{x}), \Sigma_i(\mathbf{x}))^{\pi_i}, \\ P(\mathbf{x}|\pi \otimes \mathbf{z}) = \mathcal{N}(\mathbf{x}|f(\pi \otimes \mathbf{z}), \sigma^2), \\ P(\pi \otimes \mathbf{z}) = \prod_i^m \mathcal{N}(0, 1)^{\pi_i}. \end{cases} \quad (8)$$

Similarly, we can express $h_{\mathbf{z}}$, by combining which with (7) and further inserting them into (6) we can get the following convex optimization model

$$\begin{cases} \min_{\mathbf{z}} \sum_{i=1}^m \pi_i, \\ \int_{\mathbf{z}} Q(\mathbf{z}|\mathbf{x}) \log \frac{P(\mathbf{x}|\mathbf{z})}{P(\mathbf{x}|\pi \otimes \mathbf{z})} d\mathbf{z} - \\ \mathcal{KL}[Q((\mathbf{1} - \pi) \otimes \mathbf{z}|\mathbf{x}) \| P((\mathbf{1} - \pi) \otimes \mathbf{z})] \leq \varepsilon, \end{cases} \quad (9)$$

where $\mathbf{1}$ is a m -dimensional vector with every element to be 1. Note that in the above model, the first term of the left side of the inequality constraint is closely related to the distance $|f(\pi \otimes \mathbf{z}) - f(\mathbf{z})|$ while the second term measures the \mathcal{KL} divergence between the latent variables one discards and the Gaussian noise. The former needs to be small enough so that the expectation values, $f(\pi \otimes \mathbf{z})$ and $f(\mathbf{z})$, can approach the original data \mathbf{x} , which means that the discarded units from \mathbf{z} do not contain too much information of data set. However, the latter should be large enough, which needs to discard units from \mathbf{z} as many as possible since the latent variables are i.i.d. We thus introduce a new parameter η , named gap hyperparameter, to split the constraint in (9) into two inequalities and develop a relatively relaxed optimization model

$$\begin{cases} \min_{\mathbf{z}} \sum_{i=1}^m \pi_i, \\ \int_{\mathbf{z}} Q(\mathbf{z}|\mathbf{x}) \log \frac{P(\mathbf{x}|\mathbf{z})}{P(\mathbf{x}|\pi \otimes \mathbf{z})} d\mathbf{z} \leq (1 + \eta)\varepsilon, \\ \mathcal{KL}[Q((\mathbf{1} - \pi) \otimes \mathbf{z}|\mathbf{x}) \| P((\mathbf{1} - \pi) \otimes \mathbf{z})] \geq \eta\varepsilon. \end{cases} \quad (10)$$

The solution of (10) will discard the latent variables that contain little information of data set and are also contaminated by noise heavily.

Further by introducing the Lagrange multipliers α and β , we rewrite (10) to be

$$\begin{aligned} & \min_{\mathbf{z}} L(Q, P, \pi) \\ & = \sum_i^m \pi_i + \beta \left(\int_{\mathbf{z}} Q(\mathbf{z}|\mathbf{x}) \log \frac{P(\mathbf{x}|\mathbf{z})}{P(\mathbf{x}|\pi \otimes \mathbf{z})} d\mathbf{z} - (1 + \eta)\varepsilon \right) \\ & \quad - \alpha (\mathcal{KL}[Q((\mathbf{1} - \pi) \otimes \mathbf{z}|\mathbf{x}) \| P((\mathbf{1} - \pi) \otimes \mathbf{z})] - \eta\varepsilon). \end{aligned} \quad (11)$$

We name $L(Q, P, \pi)$ by *Lagrange loss* in the context. Unlike the traditional pattern, here the Lagrange multipliers α and β are set to be hyperparameters that represent a preference of decreasing dimension or keeping information. To make the constraints of (10) be “hard” [13], a feasible selection is to set them as functions of sample \mathbf{x} , given by

$$\alpha(x) = \begin{cases} x, & x \geq 0; \\ -\infty, & x < 0, \end{cases} \quad \beta(x) = \begin{cases} +\infty, & x > 0; \\ x, & x \leq 0. \end{cases} \quad (12)$$

We will set them as some constants in the subsequent experiments.

3.2 Algorithm design and theoretical analysis

The main purpose of designing adaptive dimension reduction algorithm is to minimize the *Lagrange loss*. Note that there is only a decision variable \mathbf{z} in (11), and other parameters α , β , ε and η are set to be hyperparameters. We firstly develop algorithm to be able to pick out the optimal combination units in π for any given number of units, shown in **Algorithm 1**. In this algorithm, we consider the fixed encoder and decoder which have been trained on training set ahead of being input, and decide to keep or discard the units in latent variable vector based on the *Lagrange Loss*.

Algorithm 1 Optimization of $L(\pi)$ regarding n combination units in π

Input: $n \in [1, m]$, $L(\pi)$

- 1: $\pi = \text{ones}(m)$, a function to produce a vector with all elements to be 1;
- 2: **while** not convergent **do**
- 3: randomly generate n non-repetitive indexes, denoted by i_1, \dots, i_n ;
- 4: $\forall j \in [1, n]$ set $\pi_{i_j} = 0$ or 1, and enumerably generate 2^n vectors, labeled by $\Pi = \{\pi_1, \dots, \pi_{2^n}\}$;
- 5: **for** ξ in Π **do**
- 6: **if** $L(\xi) < L(\pi)$ **then**
- 7: $\pi = \xi$;
- 8: **end if**
- 9: **end for**
- 10: **end while**

Output: π

Theorem 1. For any $n \in [1, m]$, the Lagrange loss $L(\pi)$ in Algorithm 1 is convergent.

Proof. Since π is m -dimensional, which is finite, and its component is 0 or 1, Algorithm 1 will create a monotone sequence $L(\xi_1) > L(\xi_2) > \dots$. Also, since the function values of Lagrange loss are finite, there must exist the lowest bound, which completes the proof. \square

Let $\Pi_{m'}$ the set that contains the vectors like π and $\sum_i \pi_i = m'$. Let $\pi_{m'}$ be a m -dimensional vector whose elements are ones or zeros, and $\sum_i (\pi_{m'})_i = m'$

Theorem 2. Let Algorithm 1 converges to the $\pi_{m'}$, then when $j = m'$, $\inf_{\pi_j \in \Pi_j} h_{z \otimes \pi_j^m}$ is the local minimum in discrete interval $j \in [m' - n', m' + n']$ where $n' = \min(n, m', m - m')$

Remark 1. Algorithm 1 suggests that for any n , $L(\pi)$ or π is convergent. However, the convergent results may be quite different even though the same inputs are fed, since in Line 3 of the algorithm those n location indexes of π are generated randomly.

Remark 2. Theoretically, the appearance of the minimum Lagrange loss in Algorithm 1 may require to run it at a large n , which will be very time-consuming since each element in Π should be covered to compare all $L(\pi)$'s. A practical strategy is to implement an early stopping rule that calls the algorithm off if the Lagrange loss or the sum of π keeps unchanged for several epochs. However, the rule needs to make sure every element in π to be visited in a large probability.

For convenience, we use the expression $\text{Opt}(L(Q, P, \pi), n)$ to represent the optimization strategy of π through Algorithm 1. Then the adaptive dimension reduction algorithm, labeled by Algorithm 2, can be described as follows.

Here we use ‘‘adaptive’’ in the name of Algorithm 2. The main reason is that the algorithm, unlike other traditional dimension reduction algorithms, such as principal component analysis etc., that usually work in need of setting the result beforehand, can compute the reduced dimension adaptively according to the data sets. A further look at the above algorithm reveals that Line 2 implements Algorithm 1. As said in Remark 1, the result of Algorithm 1 is random, which may subconsciously affect the

Algorithm 2 Adaptive dimension reduction algorithm

Input: $Q(z|x)$, $P(x|z)$ (after training on training set), $\pi = \text{ones}(m)$,

$L(Q, P, \pi)$ and n

- 1: **while** not convergent **do**
- 2: $\pi = \text{Opt}(L(Q, P, \pi), n)$;
- 3: set new latent variables \tilde{z} with $\tilde{m} = \sum_{i=1}^m \pi_i$;
- 4: retrain VAE or CVAE on training set to get new $Q(\tilde{z}|x)$ and $P(x|\tilde{z})$;
- 5: $Q = Q(\tilde{z}|x)$, $P = P(x|\tilde{z})$;
- 6: $\pi = \text{ones}(\tilde{m})$;
- 7: **end while**

Output: \tilde{m}

result of Algorithm 2. However, the following theorem suggests Algorithm 2 to be convergent.

Theorem 3. Given a group of specific m and n , Algorithm 2 is convergent regardless of the randomness of the optimizer in Line 2.

Proof. The detailed proof can be found in Appendix. \square

Theorem 4. Every iteration in Algorithm 2 returns a VAE with smaller loss on training set.

Proof. Consider a random epoch in Algorithm 2, let m be the dimension of the latent variables vector z at the beginning of this epoch and m_v be the dimension of the latent variables vector v we get after this epoch, then there is a $\pi_{m_v}^m \in \Pi_{m_v}$ such that $\pi_{m_v}^m = \text{Opt}(L(Q^m, p^m, \text{ones}(m)), n)$, thus

$$h_{z \otimes \pi_{m_v}^m} - h_z \leq \epsilon$$

Without losing generality, we let $\epsilon = 0$, we have $h_{z \otimes \pi_{m_v}^m} \leq h_z$, and by the Lemma 1, we have completed the proof. \square

Remark 3. The output of Algorithm 2 is the dimension of latent variables in \tilde{M} , which is actually sensitive to the initial m and n but keeps unchanged despite performing Algorithm 1. The convergent dimension \tilde{m} of Algorithm 2 is the one nearest to the initial m satisfying $\tilde{m} \leq m$, but not sure to be the optimal one. It is possible to get a smaller \tilde{m} if a new m less than the convergent result is fed into Algorithm 2 to run it again.

3.3 Algorithms application to generate better VAE

Except for reducing the dimension of latent variables, the algorithms can be also used to generate the hidden layers of encoder and decoder in VAE, and get better VAE.

Consider an initial VAE only with a single layer of encoder (input layer), a middle layer of latent variables and a single layer of decoder (output layer). We use Algorithm 2 to generate the hidden layers in encoder and decoder in the form of symmetry. The first time of application of the algorithms will yield better dimension of the latent variables. Then we use this ‘‘better dimension’’ as the number of neural units to construct the first layer of hidden layers in encoder and decoder. Based on the new VAE (with new encode, latent variables and decoder), we make the second time of applications of Algorithm 2. The same procedures are implemented repeatedly until the number of hidden layers reach the desired value. The detailed process to generate better VAE is exhibited in Fig. 5.

Noticeably, the above ‘‘better VAE’’ is generated in a greedy way. During every time of applying Algorithm 2, the neural units

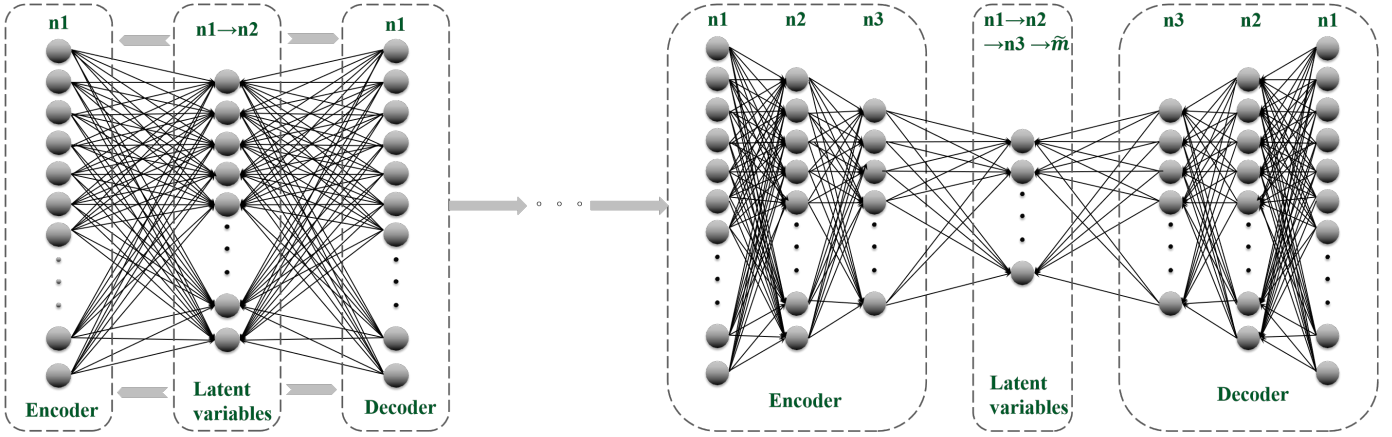


Fig. 5: The generation process of VAE through applying **Algorithm 2**.

in the hidden layers of encoder and decoder are generated as few as possible. A potential advantage of this generation pattern is that the generated VAE has fast forwarding speed and weak overfitting phenomenon.

4 EXPERIMENTAL STUDIES AND DISCUSSIONS

TABLE 1: Basic information about six data sets

Name of data set	Number of pictures	Number of pixels on one picture
MNIST	70000	28×28
FashionMNIST	70000	28×28
ATTfaces	400	112×92
Covid-19	306	1000×1000
CACD	163446	250×250×3
CAT	9000	500×375×3

MNIST: handwritten digits; FashionMNIST: images of clothes; ATTfaces and CACD: human face pictures; Covid-19: images of x-ray in different condition; CAT: cat face pictures.

In this section, we use 6 data sets to evaluate our algorithms, including MNIST, FashionMNIST, ATTfaces¹, Covid-19², CACD [14] and CAT³. The basic information about them is listed in Table 1. In terms of the numbers of pictures and of pixels in one picture, we sort the first two data sets as small-sized data sets, the middle two data sets as middle-sized data sets while the last two as large-sized data sets. All data sets are used to test the algorithms on VAE while only the data sets of MNIST and Covid-19 are employed on CVAE. The initial dimensions of latent variables for every data set depend on the number of pixels on one image, which are given in Table 2. We also provide the values of all hyperparameters used in the models, and the setting of the training set and testing set in this table. Here, the hyperparameters α and β are set around the initial dimension of latent variables for the purpose of making a balance between dimension reduction and information reservation.

4.1 Experimental results of VAE

In this subsection, the reduction dimension algorithm is applied to the VAE model. For the small-sized data sets, we use DNN to con-

struct the encoder and decoder of VAE. With those experimental setups reported in Table 2, **Algorithm 2** is implemented on their training sets, respectively, and outputs the optimal dimension of latent variables to be 22 for MNIST and 15 for FashionMNIST. The comparisons between the initial dimension and the optimal one are displayed in Table 3. It is clear that the proposed algorithms can reduce the dimension of latent variables greatly, both from the initial 100 to the current low values. These results imply a large possibility that there will be serious overfitting phenomena in the models with 100-dimensional latent variables. To observe these phenomena, we further make experiments on the testing sets of these two data sets using the VAE models with latent variables of initial dimension, convergent dimension and others. The dimensions selection in the experiments is in large gaps at the beginning stage of initial dimension while in small gaps whilst being close to the convergent dimension. The reason is that the change of dimension will have a little effect on the model if it is far away from the convergent dimension. Shown in Table 4 are the results, where the “Loss” items are computed according to (7) and (8). As can be seen from this table, the “Loss” values at the initial dimensions are apparently lower than those at the convergent dimensions. Moreover, the latter reach the lowest compared with other cases, being 69.6778 and 64.8587, respectively. Another noticeable point is that when the dimensions of latent variables continue to decrease from the convergent dimensions, the corresponding “Loss” values will increase, which means the models will become underfitting. At this point, the convergent dimensions seem to be the “turning points” to distinguish overfitting and underfitting of VAE in modelling the data sets of MNIST and FashionMNIST. This conversely indicates that **Algorithm 2** can work effectively for weakening overfitting phenomenon through reducing dimension of latent variables in the VAE model.

1. <https://www.r-bloggers.com/wp-content/uploads/2010/09/ATTfaces.tar.gz>
 2. <https://www.kaggle.com/pranavraikokte/covid19-image-dataset/metadata>
 3. <https://www.kaggle.com/crawford/cat-dataset>

TABLE 2: Experimental setups for six data sets

Model	Data set	Hyperparameters				Initial dimension of latent variables	Training set size vs. Testing set size
		α	β	η	ϵ		
VAE	MNIST	100	75	3	0.1	100	6:1
	FashionMNIST	100	75	3	0.1	100	6:1
	ATTfaces	2000	1800	1	1	2000	9:1
	Covid-19	100	80	1	1	100	4:1
	CACD	3000	2800	1	0.1	800	24:1
	CAT	50	40	1	0.1	100	8:1
CVAE	MNIST	100	80	3	0.1	100	6:1
	Covid-19	1000	800	1	0.1	100	4:1

TABLE 3: Comparisons between the initial dimension and the convergent one of latent variables on six data sets

Model	Data set	VAE					CVAE		
		MNIST	FashionMNIST	ATTfaces	Covid-19	CACD	CAT	MNIST	Covid-19
Initial		100	100	2000	100	800	100	100	100
Convergent		22	15	100	4	40	19	4	5

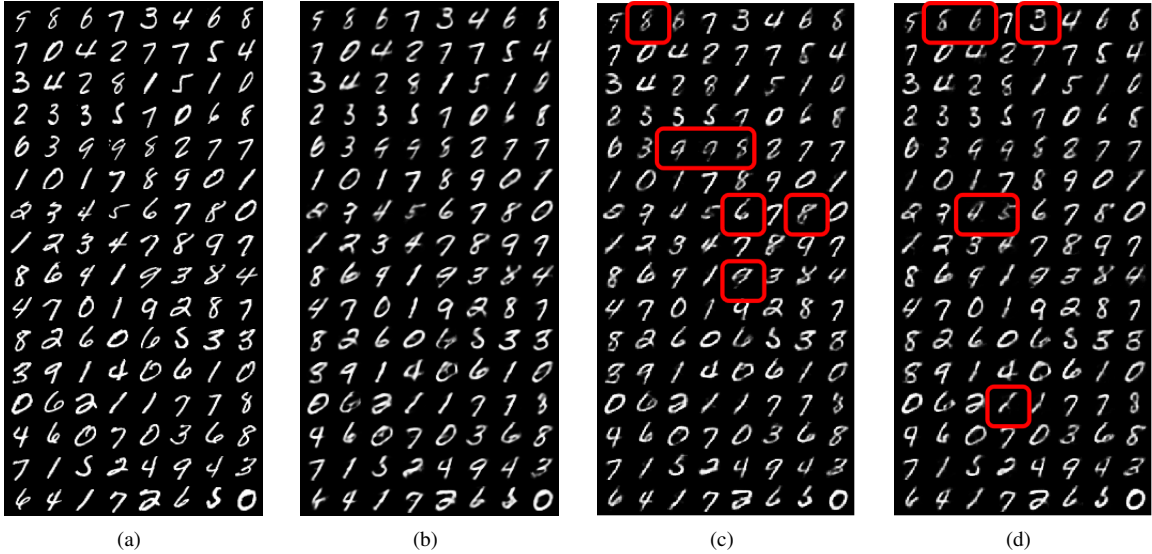


Fig. 6: MNIST images generated by the VAE models with different latent variables: (a) original images; (b) 22 dimensions (convergent); (c) 50 dimensions; (d) 100 dimensions. The red frames identify some unclear parts of images. The same mark is used in Figs. 7, 8, 9 and 11 with the same meaning.

TABLE 4: Testing results of VAE on MNIST and FashionMNIST at different dimensions of latent variables

MNIST		FashionMNIST	
Dimension	Loss [†]	Dimension	Loss [†]
100	74.1638	100	68.1159
80	73.3230	80	69.2199
70	72.5838	70	67.1504
60	72.1105	60	67.1762
50	73.9732	50	67.8204
40	72.0187	40	67.4163
30	70.2824	30	65.0471
22[§]	69.6778[§]	20	65.6899
20	70.2290	15[§]	64.8587[§]
10	75.9148	10	66.8908

[†] “Loss” represents the loss function of VAE which is minus of right part of (2) evaluated on the testing set; [§]The bold represents the results are yielded at the convergent dimension. The above two pieces of descriptions also apply to Tables 5, 6 and 7.

TABLE 5: Testing results of VAE on ATTfaces and Covid-19 at different dimensions of latent variables

ATTfaces		Covid-19	
Dimension	Loss [†]	Dimension	Loss [†]
2000	4646.1689	100	440538.0312
800	5250.0884	80	446455.8438
700	5260.8203	70	455817.3125
600	4687.7856	60	530468.6875
500	5556.7773	50	503117.2812
400	6118.9741	40	466038.4375
300	5914.4434	30	379977.5625
200	5717.3677	20	424810.0312
150	5324.4092	15	447669.2188
105	5187.8164	10	458102.1562
100[§]	4322.5444[§]	4[§]	339562.6562[§]
50	4500.3042	2	436385.90621

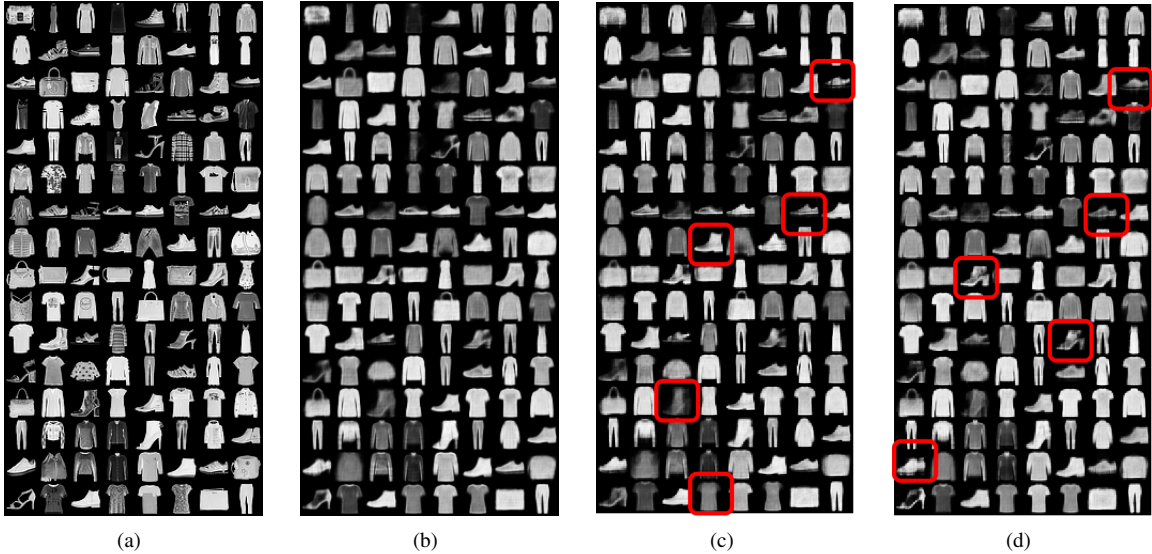


Fig. 7: FashionMNIST images generated by the VAE models with different latent variables: (a) original images; (b) 15 dimensions (convergent); (c) 50 dimensions; (d) 100 dimensions.

To observe the effect of **Algorithm 2** more visually, we use the trained VAE model to generate new images at some different dimensions of latent variables, especially at the convergent dimension, with the results shown in Figs. 6 and 7 for MNIST and FashionMNIST, respectively. As can be seen from these two figures, at the convergent dimensions the generated images look very clear (sub-figures (b)), nearly approaching the original images (sub-figures (a)). However, at other dimensions, the generated images look not so clear (sub-figures (c) and (d)), and there exist some blurry parts in the images, identified by the red frames. These observations confirm again that **Algorithm 2** is quite valid in improving the VAE model precision through reducing the dimension of latent variables.

Following the same procedures, we continue to test **Algorithm 2** on the middle-sized (ATTfaces and Covid-19) and large-sized (CACD and CAT) data sets given in Table 1. The experimental setups are also presented in Table 2. Since the pixels on one picture is rather high for these sample sets, to save space and time we use convolutional neural network (CNN) and ReLU activation function to construct the encoder, and transposed convolution neural network (TCNN) to construct the decoder in the VAE model. Table 3 reports the convergent results for these four data sets, being 100, 4, 40 and 19, respectively. It is amazing to notice that there is significant decrease from the initial dimension to the convergent dimension for ATTfaces, Covid-19 and CACD, especially for Covid-19, the decrease from 100 to 4 attaining 25 times. This will bring a good result that the training time of the VAE model will reduce dramatically. We also evaluate the results of **Algorithm 2** using the testing sets of these four data sets. The results are displayed in Tables 5 and 6. As one may expect, the VAE models still have the best performance at the convergent dimension of latent variables for middle-sized and large-sized data sets. Similarly, we use the trained VAE models to generate new ATTfaces and Covid-19 images at different dimensions of latent variables, exhibited in Figs. 8 and 9. The results show again that the images generated at the convergent dimensions approach the original images most (sub-figures (b)) while other cases contains

too many unclear parts, especially like Fig. 8(c), Fig. 9(c)(d), nearly the whole pictures being unclear. Hence, **Algorithm 2** is still quite strong to handle middle-sized and large-sized data sets under consideration.

TABLE 6: Testing results of VAE on CACD and CAT at different dimensions of latent variables

CACD		CAT	
Dimension	Loss [†]	Dimension	Loss [†]
800	107977.4453	100	310707.5000
700	117547.9688	70	327680.2188
600	100867.4531	60	324024.2188
500	111773.3125	50	334639.5312
400	109225.4609	40	324773.5312
300	105882.0703	30	305162.6250
200	109955.7734	20	304568.1250
100	95690.7578	19[§]	268931.7500[§]
50	112495.2422	15	294182.7812
40[§]	94860.6016[§]	10	348134.4688
20	97928.5234	6	305552.1875

Finally, we use **Algorithm 2** to generate better VAE through learning the data set of MNIST according to the procedures described in Section 3.3. We begin the application experiments with the initial dimension of latent variables to be 450. After the first round of running **Algorithm 2**, we get the convergent dimension of latent variables to be 272. We put 272 neural nodes both into the encoder and decoder to construct the first layer of hidden layer therein. Then we use the new VAE model with new encoder, 272-dimensional latent variables and new decoder to begin the second round of applying **Algorithm 2**. The resulting convergent dimension is 24, at which we further get the “Loss” on the testing set to be 69.664. This value is a little less than the best result “69.6778” reported in Table 4, which corresponds to the VAE model with a layer of 400-dimensional hidden layer in the encoder and decoder, and 22-dimensional latent variables. We also

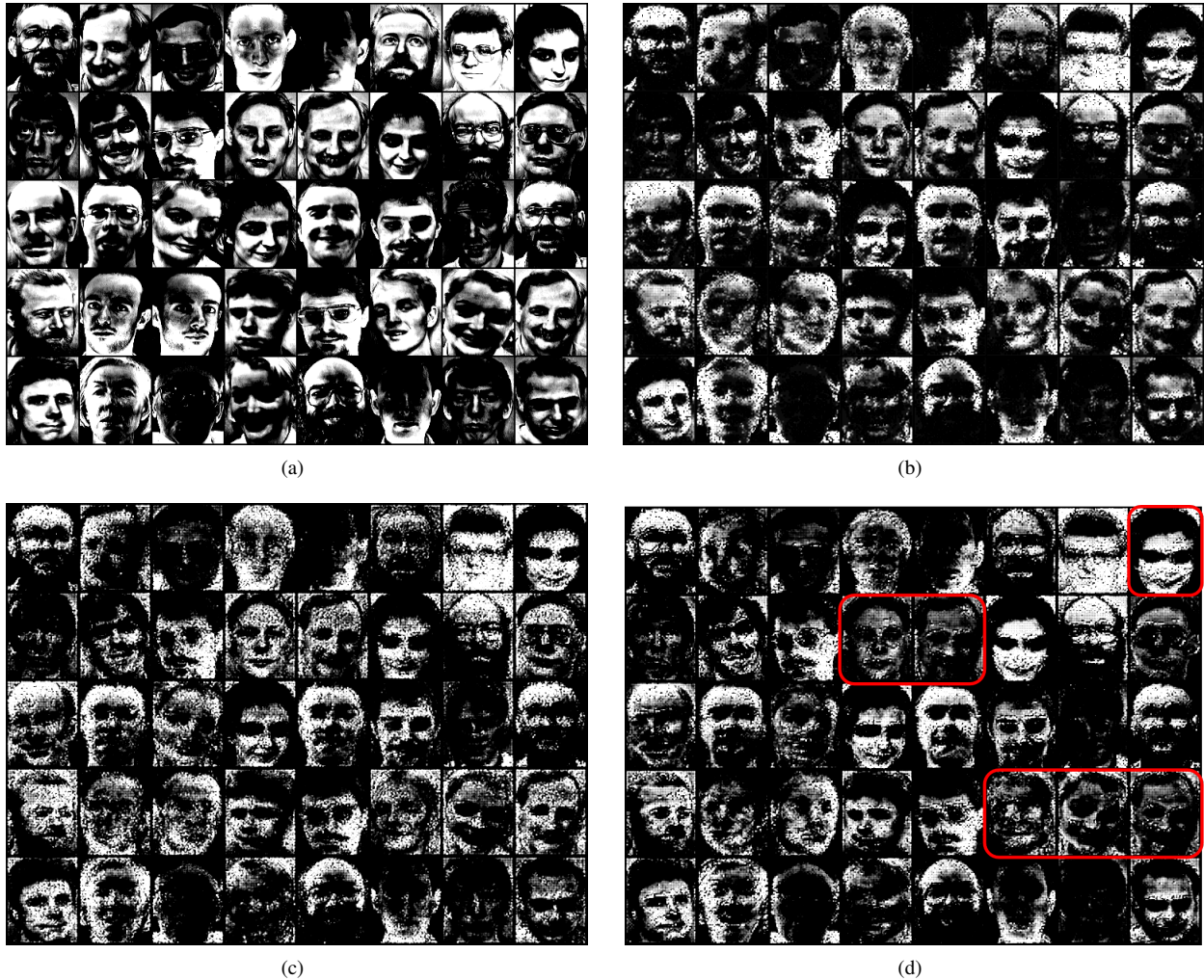


Fig. 8: ATTFaces images generated the VAE models with different latent variables: (a) original images; (b) 100 dimensions (convergent); (c) 150 dimensions; (d) 400 dimensions.

provide the image generated by the new better VAE model in Fig. 9, from which the image generated by this new model (subfigure (b)) looks more clear than other one (subfigure (c)).

Note that from the viewpoint of technique, this application just uses the adaptive dimension reduction algorithm based on a greedy strategy, so it is still possible to have a better combination of different layers in the model.

4.2 Experimental results of CVAE

In this subsection, the CVAE model works for validating the reduction dimension algorithm, which, unlike VAE, is supervised learning. Every image is thus assigned a label beforehand, and the loss function, the optimization model, and the *Lagrange loss* are quite similar to those for VAE, just adding the label information \mathbf{y} in the corresponding conditions of probability expressions. Here, we use one-hot encoding to represent the label of each image, so there are two vectors in the latent layer, i.e., the latent variables and the labels. In this case, only two data sets, a small-sized MNIST and a middle-sized Covid-19, are considered.

For the MNIST data set, each image is assigned a number, ranging from 0 to 9, as the label, i.e., the dimension of one-hot encoding is 10, which is fixed in the latent layer. And for

Covid-19, a three classification task is designed, i.e., each image is labeled by a patient with Covid-19, a patient with other disease or a healthy patient. We use the parameters given in Table 2 and the initial dimension presented in Table 3, then we get the convergent dimension to be 4 and 5 for these two data sets, also exhibited in Table 3, after applying **Algorithm 2** to CVAE. Further, we make some comparison experiments through testing sets between the CVAE models at the convergent dimensions and at others. The results are reported in Table 7. Also, as one might expect, the optimal results appear at the convergent dimension. In addition, the generated MNIST and Covid-19 images, shown in Figs. 11 and 12, respectively, support this point likewise. Hence, **Algorithm 2** witnesses success again for CVAE working on the used data sets.

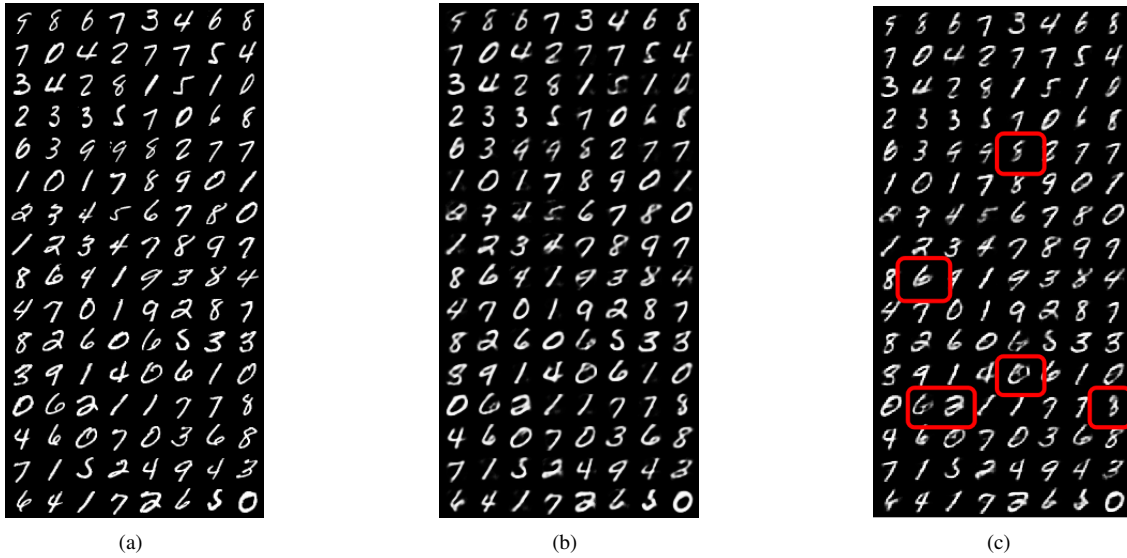


Fig. 9: MNIST images: (a) original image, the same to Fig. 6(a); (b) generated by the new better VAE model; (c) the same to Fig. 6 (b).

TABLE 7: Testing results of CVAE on MNIST and Covid-19 at different dimensions of latent variables

MNIST		Covid-19	
Dimension	Loss [†]	Dimension	Loss [†]
100	28.6498	100	460397.3438
80	28.2854	80	531166.5625
70	28.0323	70	461905.8125
60	27.3108	60	521487.5938
50	27.0910	50	428283.6875
40	26.7257	40	493133.9062
30	26.8649	30	555563.6250
20	26.4686	20	565356.6250
10	26.3910	15	442531.8438
5	26.2822	10	442047.6875
4[§]	25.9880[§]	5[§]	301410.6875[§]
2	28.9239	3	540075.1250

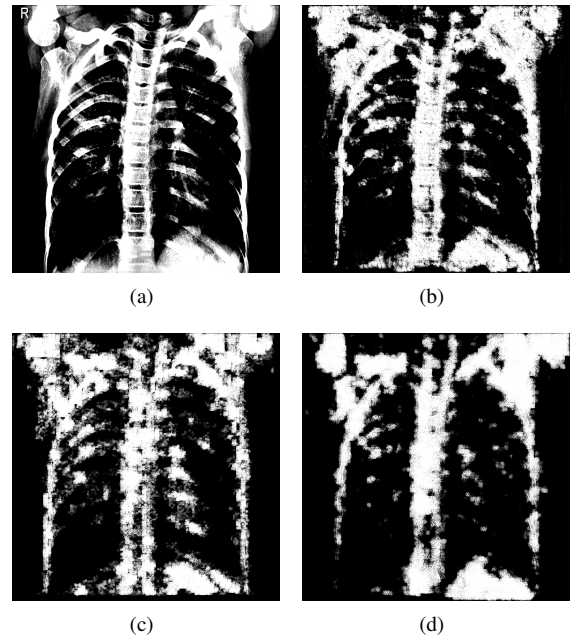


Fig. 10: Covid-19 images generated by the VAE models with different latent variables: (a) original images; (b) 4 dimensions (convergent); (c) 50 dimensions; (d) 100 dimensions.

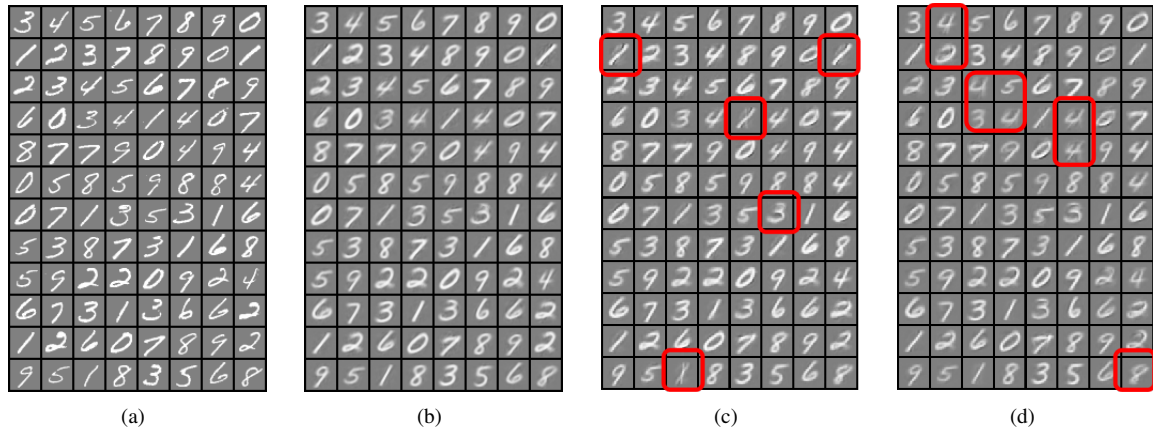


Fig. 11: MNIST images generated by the CVAE models: (a) original images; (b) 22 dimensions (convergent); (c) 50 dimensions; (d) 70 dimensions.

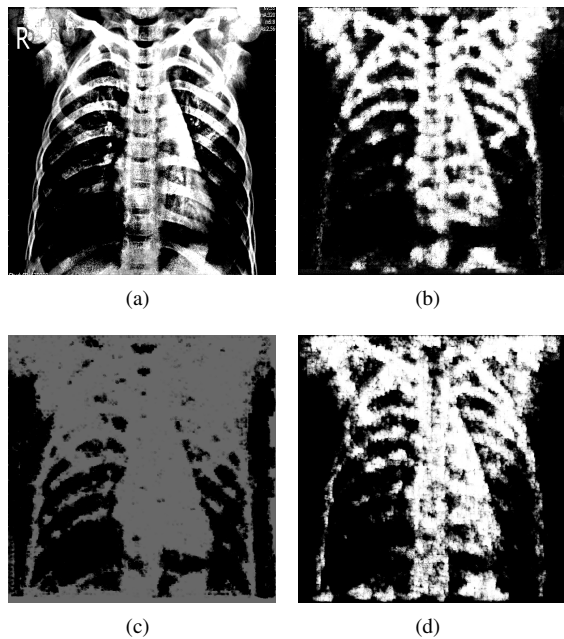


Fig. 12: Covid-19 images generated by the CVAE models with different latent variables: (a) original images; (b) 5 dimensions (convergent); (c) 50 dimensions; (d) 100 dimensions.

4.3 Discussions

GAN, the most famous generative model, has the discriminator which is to distinguish fake images and original images, and the generator which is to generate fake images. GAN uses the minimax game as the loss function to train the discriminator and generator [2]. We want to use stochastic gradient descent (SGD) to reach the Nash equilibrium in this minimax game, which is unstable and needs more computation resources compared to VAE.

Instead of training a generator directly, VAE combines the encoder and decoder as a generator which gives more interpretability to the fake images. But VAE gives a strong assumption to the distribution of fake images, i.e. every pixel is independent with each other, in my opinion, this strong assumption makes fake images less clear than the images generated by GAN.

Most importantly, VAE can generate specific images we want, however the generating process of GAN is that it takes Gaussian noise as an input and generates images randomly, it indicates that this process is totally uncontrollable.

5 CONCLUSION

In conclusion, we introduce an adaptive algorithm that can automatically learn the dimension of the latent variable without using the validation set, we spend most of the computation time on computing the Lagrange loss, which needs forward propagation only, the algorithm also needs us to re-train our model once we get the first optimization on layers' dimension, it needs to re-train a few times until the dimension converges, the bigger the dimension the layers have, the faster the number of its units decreases. The algorithm returns the sum of the π_i , and the π which the algorithm converges is a vector with zero or one elements, that also makes certain explanatory on DNN: The zero element represents the unit it multiplies in the latent variable contains too much noise and we inactivate it; otherwise, we activate the units which relate to the one elements in π .

We only use the adaptive dimension reduction algorithm on VAE or its variants, but you may find that we barely use the characters of variational autoencoders in whatever the proof or the algorithm! In fact, on a simple DNN or RNN model we have a loss function f , you can put the π on whatever layer you like (you even can put the π on every layer, then all we need to do is minimizing the sum of π_i under the constraint of (6) and that is exactly what we do on VAE, that means the model with DNN or RNN can also use this technique.

APPENDIX: PROOFS OF SOME RESULTS

A. Proof of Theorem 3

B. Proof of Theorem

Proof of theorem 2

Proof. Let $\pi_{m'}^m = \text{Opt}(L(\text{ones}(m)), n)$ where $\pi_{m'}^m \in \Pi_{m'}$. Since $\pi_{m'}^m$ is unchanged after enough epochs, for $i=1, 2, \dots, \min(n, m', m-m')$

$$h_{z^m \otimes \pi_{m'}^m} - h_{z^m} \leq \epsilon$$

$$h_{z^m \otimes \pi_{m'+i}^m} - h_{z^m} \leq \epsilon \text{ or } h_{z^m \otimes \pi_{m'+i}^m} - h_{z^m} \geq \epsilon,$$

where $\pi_{m'+i}^m \in \Pi_{m'+i}$. By the assumption, we get $h_{z^m \otimes \pi_{m'}^m} < h_{z^m \otimes \pi_{m'+i}^m}$. The units of latent variables which is related to zeros are considered as noise and the units which related to ones are considered contain information, thus the equality is achieved for any $\pi_{m'}^m$, then

$$h_{z^m \otimes \pi_{m'}^m} \leq \inf_{\Pi_{m'+i}} h_{z^m \otimes \pi_{m'+i}^m} \quad (13)$$

In another hand, for any $\pi_{m'-i}^m \in \Pi_{m'-i}$,

$$h_{z^m \otimes \pi_{m'-i}^m} - h_{z^m} > \epsilon.$$

Therefore, $h_{z^m \otimes \pi_{m'}^m} \leq h_{z^m \otimes \pi_{m'-i}^m}$, by the arbitrariness of $\pi_{m'-i}^m$, we have

$$h_{z^m \otimes \pi_{m'}^m} < \inf_{\pi_{m'-i}^m \in \Pi_{m'-i}} h_{z^m \otimes \pi_{m'-i}^m}. \quad (14)$$

Combining the equation (14),(15) and the fact that $\inf_{\pi_{m'}^m \in \Pi_{m'}} h_{z^m \otimes \pi_{m'}^m} \leq h_{z^m \otimes \pi_{m'}^m}$, we have proved the theorem. \square

Proof of theorem 3

Proof. First of all, we assume that the $Q(\mathbf{z}|\mathbf{x}), P(\mathbf{x}|\mathbf{z})$ have been trained on the training set and have the same parameters as $Q(\pi \otimes \mathbf{z}|\mathbf{x}), P(\mathbf{x}|\pi \otimes \mathbf{z})$ do.

we use \mathbf{z}^i to represent the latent variable whose dimension is i

It is easy to prove that $m = 0$ can not be the convergent dimension since $m = 0$ means no data are passed to the decoder, the fake data generated by the decoder is all noise and the equation (5) can not be achieved, so if we set \mathbf{z}^1 as the initial latent variable, it will not decrease anymore. Since the \mathbf{z}^i is finite, there is a integer s such that $\dim \mathbf{z}^{s+1}$ as the initial latent variable is changeable and \mathbf{z}^s is unchangeable. That is to say the **Algorithm 2** is convergent

We assume that we run the **Algorithm 1** two times and have different convergent vector π_s^t and π_u^t . Therefore

$$\begin{aligned} h_{z^t \otimes \pi_s^t} - h_{z^t} &\leq \epsilon \\ h_{z^t \otimes \pi_u^t} - h_{z^t} &\leq \epsilon. \end{aligned}$$

Without loss of generality, we assume $s - u < n$, since if $s - u > n$, there exists a s' such that $s > s' > u$, $s - s' < n$ and $h_{z^t \otimes \pi_{s'}^t} - h_{z^t} \leq \epsilon$.

By the assumption in section 2, we have $h_{z^t \otimes \pi_u^t} < h_{z^t \otimes \pi_{s'}^t}$. But by the proof in **Theorem 2**, since $s - u < n$, $h_{z^t \otimes \pi_s^t} \leq \inf_{\pi_u^t \in \Pi_u} h_{z^t \otimes \pi_u^t}$. It is a contradiction. \square

ACKNOWLEDGMENTS

This work was funded by the National Nature Science Foundation of China under Grant 12071428 and 11671418, and Zhejiang Provincial Natural Science Foundation of China under Grant No. LZ20A010002.

REFERENCES

- [1] D. P. Kingma and M. Welling, "Auto-encoding variational bayes," *CoRR*, vol. abs/1312.6114, 2014.
- [2] I. Goodfellow, J. Pouget-Abadie, M. Mirza, B. Xu, D. Warde-Farley, S. Ozair, A. C. Courville, and Y. Bengio, "Generative adversarial nets," in *NIPS*, 2014.
- [3] I. T. Jolliffe and J. Cadima, "Principal component analysis: a review and recent developments," *Philosophical Transactions of the Royal Society A: Mathematical, Physical and Engineering Sciences*, vol. 374, no. 2065, p. 20150202, 2016.
- [4] K. Sohn, H. Lee, and X. Yan, "Learning structured output representation using deep conditional generative models," in *NIPS*, 2015.

- [5] J. Walker, C. Doersch, A. Gupta, and M. Hebert, "An uncertain future: Forecasting from static images using variational autoencoders," *ArXiv*, vol. abs/1606.07873, 2016.
- [6] Q. Liu and D. Wang, "Stein variational gradient descent: A general purpose bayesian inference algorithm," in *NIPS*, 2016.
- [7] Y. Pu, Z. Gan, R. Henao, C. Li, S. Han, and L. Carin, "2 stein learning of variational autoencoder (stein vae) 2," 2017.
- [8] I. Higgins, L. Matthey, A. Pal, C. Burgess, X. Glorot, M. Botvinick, S. Mohamed, and A. Lerchner, "beta-vae: Learning basic visual concepts with a constrained variational framework," 2016.
- [9] J. Platt, "Sequential minimal optimization : A fast algorithm for training support vector machines," *Microsoft Research Technical Report*, 1998.
- [10] C. Doersch, "Tutorial on variational autoencoders," *ArXiv*, vol. abs/1606.05908, 2016.
- [11] M. J. Johnson, D. K. Duvenaud, A. Wiltchko, R. P. Adams, and S. R. Datta, "Composing graphical models with neural networks for structured representations and fast inference," *Advances in neural information processing systems*, vol. 29, pp. 2946–2954, 2016.
- [12] D. Koller and N. Friedman, *Probabilistic graphical models: principles and techniques*. MIT press, 2009.
- [13] S. Boyd, S. P. Boyd, and L. Vandenberghe, *Convex optimization*. Cambridge university press, 2004.
- [14] B.-C. Chen, C.-S. Chen, and W. H. Hsu, "Cross-age reference coding for age-invariant face recognition and retrieval," in *Proceedings of the European Conference on Computer Vision (ECCV)*, 2014.